Controllable all-fiber orbital angular momentum mode converter

Article *in* Optics Letters · September 2015

DOI: 10.1364/OL.40.004376

CITATIONS
230

READS
1,338

5 authors, including:

Shuhui Li
Huazhong University of Science and Technology
70 PUBLICATIONS **1,808** CITATIONS
SEE PROFILE

Qi Mo
Raycus Fiber Laser Technologies Co., Ltd/ Brightcore Specialty Fiber.
86 PUBLICATIONS **1,751** CITATIONS
SEE PROFILE

Cheng Du
Beijing University of Civil Engineering and Architecture
72 PUBLICATIONS **3,552** CITATIONS
SEE PROFILE

Jian Wang
Huazhong University of Science and Technology
7 PUBLICATIONS **456** CITATIONS
SEE PROFILE

Optics Letters

Controllable all-fiber orbital angular momentum mode converter

Shuhui Li,[1] Qi Mo,[2] Xiao Hu,[1] Cheng Du,[2] and Jian Wang[1,*]

[1]Wuhan National Laboratory for Optoelectronics, School of Optical and Electronic Information, Huazhong University of Science and Technology, Wuhan 430074, Hubei, China
[2]Fiberhome Telecommunication Technologies Co. Ltd, Wuhan 430074, China
*Corresponding author: jwang@hust.edu.cn

Received 8 July 2015; revised 13 August 2015; accepted 26 August 2015; posted 27 August 2015 (Doc. ID 245564); published 15 September 2015

We present a scheme to realize a controllable, scalable, low-cost, and versatile all-fiber orbital angular momentum (OAM) converter. The converter consists of a two-mode fiber (TMF) with its input terminal welded with a single-mode fiber, a mechanical long-period grating (LPG), a mechanical rotator, metal flat slabs, and a fiber polarization controller. The LPG is employed to convert the fundamental fiber mode to higher-order modes and the flat slabs are used to stress the TMF to adjust the relative phase difference between two orthogonal higher-order modes. Selective conversion from the LP_{01} mode to the LP_{11a}, LP_{11b}, OAM_{-1}, or OAM_{+1} mode is demonstrated in the experiment.

OCIS codes: (060.2340) Fiber optics components; (050.4865) Optical vortices; (060.2330) Fiber optics communications; (060.4230) Multiplexing.

http://dx.doi.org/10.1364/OL.40.004376

Structured light beams have received great attention in recent years. Optical beams having complex phase, intensity, or polarization structures all belong to structured lights. Structured lights have been used in a wide amount of applications, such as atom tapping, tweezers, subwavelength resolution nano-optics, nanofabrication, laser cooling, quantum informatics, and optical communications [1]. An optical vortex is a typical structured light. An optical vortex with a phase singularity is characterized by a helical phase front of $\exp(il\varphi)$, in which φ refers to the azimuth angle and l is the topological charge number [2]. Because of the helical phase structure, the light wave at the axis cancels out, giving rise to a phase singularity at which the phase is indeterminate and the amplitude is zero. In 1992, Allen *et al.* indicated that for beams with helical phase fronts of $\exp(il\varphi)$, the orbital angular momentum (OAM) in the propagation direction has the discrete value of $l\hbar$ per photon, where $\hbar$ is the reduced Planck constant [3]. Since the recognition of an optical vortex carrying OAM, many new research areas have been accelerated, ranging from optical manipulation to high-dimensional quantum entanglement [4–7]. Very recently, the optical vortex, also called an OAM beam, has attracted great attention for increasing transmission capacity and spectral efficiency in optical communication systems [8–12].

Driven by their distinctive properties and miscellaneous applications, there have been many attempts to generate and manipulate OAM beams. Such attempts include cylindrical lens mode converters, q-plates, spiral phase plates, spatial light modulators (SLM), metamaterials-based phase plates, and silicon integrated devices [3,13–16]. Typically, the most widely used one is the SLM together with some accessory elements, which are generally expensive. Meanwhile, there is an increasing interest in the generation of OAM beams with optical fibers [17–20]. A laudable goal would be to design a scalable all-fiber OAM converter which can controllably convert a fiber fundamental mode to an OAM beam.

In this Letter, we propose a scalable method to realize a controllable all-fiber OAM converter. The converter consists of a two-mode fiber (TMF) with its input terminal spliced with a single-mode fiber (SMF), a mechanical long-period grating (LPG), a mechanical rotator, metal flat slabs, and a fiber polarization controller. By adjusting (stressing, rotating, and twisting) the above mechanical devices, one can selectively convert an input LP_{01} mode from the SMF to the LP_{11a}, LP_{11b}, OAM_{-1}, or OAM_{+1} mode at the output terminal of the TMF. To verify the charge of the generated OAM beams, interference between the OAM beam and a reference Gaussian beam is recorded.

For a conventional multimode optical fiber which meets the weak-guidance approximation conditions, the electric fields can be obtained by solving the scalar wave equation yielding the familiar linearly polarized (LP) modes. There are two indices to describe a LP_{lm} mode, where l refers to the azimuthal index and m refers to the radial index. The $LP_{l>0m}$ modes have degenerate odd and even forms sometimes labeled a and b. As an example, the intensity and phase profiles of LP_{11a} and LP_{11b} are depicted in Fig. 1. Fiber OAM modes can be obtained by combining the degenerate odd and even LP_{lm} mode with $\pm\pi/2$ phase difference (i.e., $OAM_{\pm l} = LP_{lma} \pm i \times LP_{lmb}$). The annular intensity and helical phase profiles of $OAM_{\pm 1}$ composited by LP_{11a} and LP_{11b} are illustrated in Fig. 1. However, if there is no phase difference between odd and even modes, the combining result ($LP_{lma} \pm LP_{lmb}$) is still a LP_{lm} mode which

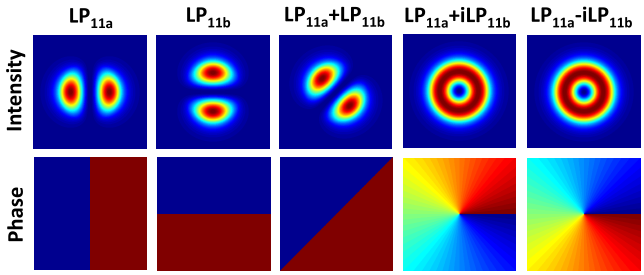

Fig. 1. Relationship between the $OAM_{\pm 1}$ mode and the LP_{11} mode.

rotates an angle compared to LP_{11a} (or LP_{11b}), as shown in Fig. 1. In order to generate OAM modes in weakly guiding fibers, production of a $\pm\pi/2$ phase difference between the odd and even LP_{lm} mode becomes a key issue. McGloin *et al.* proposed a simple method to generate the phase difference, i.e., stress the used fiber with rectangular lead weights [17]. With introduced breaking of the original rotation symmetry of the used fiber by external pressure, mode degeneracy appears to split, resulting in different transmission speed between the original degenerate odd and even modes. A $\pm\pi/2$ phase difference could be obtained with the control of the fiber length and pressure. However, in their scheme, the input beam should be a HG_{10} mode which means that it cannot directly convert a fundamental mode to higher-order OAM modes. Moreover, the scheme is not an all-fiber system which is not conducive to system integration. Therefore, we introduce a fiber grating to realize an all-fiber OAM converter.

The principle of the controllable all-fiber OAM converter is displayed in Fig. 2. A standard SMF as a mode filter is directly spliced onto a few-mode fiber (FMF), forming a whole fiber. An input LP_{01} mode from the SMF can excite the LP_{01} mode in the FMF with low insertion loss and high mode purity. Then the LP_{01} mode is converted to the LP_{11} mode by a LPG. The simplest way to make a LPG is to stress the fiber between mechanical gratings [21], as shown in Fig. 2. Moreover, a LPG can also be realized by exposing the fibers to an ultraviolet (UV) laser, a heat source, or a CO_2 laser [22–24]. By adjusting the rotator, the generated LP_{11} modes can be aligned to different directions. For the case of the LP_{11} mode aligned at 45° to the x axis of the fiber cross section, this can be expressed as a superposition of two in-phase orthogonal LP_{11} modes (e.g. LP_{11a} and LP_{11b}). When the two in-phase orthogonal modes pass through a short-length FMF stressed by a pair of flat slabs of which the stress axis is supposed to coincide with the y axis of the fiber cross section, a phase difference may appear between the two orthogonal modes. This is because the stress changes the effective dimensions of the FMF resulting in different

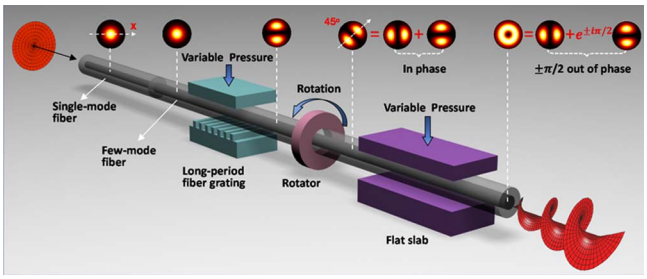

Fig. 2. Principle of the controllable all-fiber OAM beam converter.

phase velocities of the two modes. By adjusting the pressure appropriately, the two orthogonal modes can achieve a $\pm\pi/2$ phase difference at the end of the FMF, and the output is an OAM beam with a circularly symmetric annular intensity profile and a helical phase front of $\exp(\pm i\varphi)$. Remarkably, the device has versatile functions. Switching between the LP_{11a}, LP_{11b}, OAM_{-1}, and OAM_{+1} modes can also be achieved by adjusting the rotator and pressure loaded on the flat slab.

The FMF employed in this work is a custom-designed step-index TMF with a core diameter of 15 μm and a 0.336% refractive index difference between the core and cladding. The fiber is optimized to stably support LP_{01} and LP_{11} mode transmission. The calculated effective refractive indices of the LP_{01} and LP_{11} modes of the deigned TMF as a function of wavelength λ are depicted in Fig. 3. In order to realize mode coupling between the LP_{01} and LP_{11} modes, the period (Λ) of the LPG should be equal to the modal beat length, i.e $\Lambda = \lambda/(n_{01} - n_{11})$, where n_{01} and n_{11} are the effective refractive indices of the two modes. The calculated grating period for mode coupling between the LP_{01} and LP_{11} modes versus wavelength is also shown in Fig. 3. At 1550 nm, the grating period is estimated to be 833 μm. To cover the whole C- and L-bands (from 1530 to 1625 nm), the grating should have a dynamic adjustment range of 822–837 μm. The top view of the designed mechanical LPG is illustrated in Fig. 4. The effective period can be changed by varying the angle of the grating relative to the fiber. The LPG is designed with an initial tilt angle α_0. When the fiber is aligned to the horizontal direction, the effective period is Λ_1. When the fiber is aligned to the "Λ_-" direction, the effective period decreases, and the minimum value is Λ_0. When the fiber is aligned to the "Λ_+" direction,

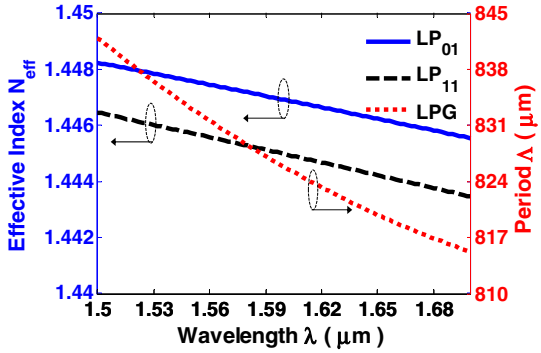

Fig. 3. Modal effective indices for the LP_{01} and LP_{11} modes of the custom-designed TMF. Calculated period of the LPG for mode coupling between the LP_{01} and LP_{11} modes.

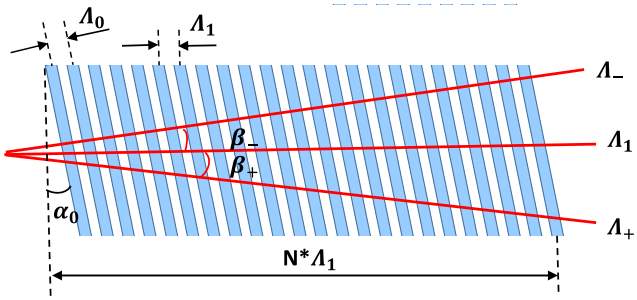

Fig. 4. Structure of the mechanical LPG.

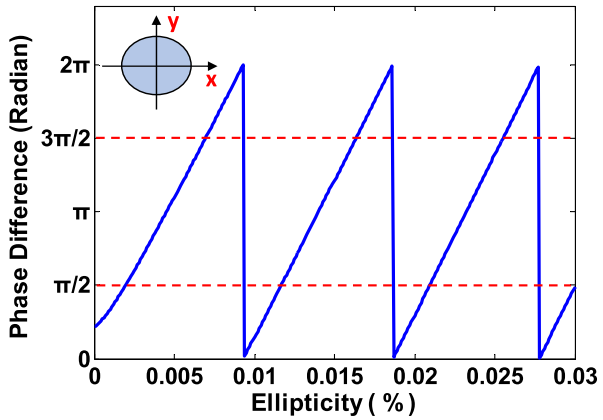

Fig. 5. Phase difference between two orthogonal LP_{11} modes versus ellipticity of the fiber core. The TMF is 75 mm long.

the effective period increases. In order to guarantee the adjusting regulation range, the used Λ_1 and Λ_0 are about 835 and 810 μm, respectively. The number of the grating period N is 30, which is beneficial to provide high coupling with acceptable bandwidth and favorable stability [21].

In order to achieve flexible control of the phase difference between the two orthogonal modes, a pair of 75 mm metal flat slabs is selected to stress the TMF. The relationship between the fiber deformation caused by the stress and the phase difference can be described by a simple elliptical core model, as shown in Fig. 5. The y direction is the direction of stress. The ellipticity of the fiber core increases when increasing the pressure. Figure 5 shows the phase difference between two orthogonal LP_{11} modes as a function of ellipticity of the core. It can be seen that, with the increase of pressure, the phase difference appears as a cyclical change. This kind of cyclical change is beneficial to phase difference adjustment and selective mode generation, due to the multiple values of pressure corresponding to the same phase difference. When the phase difference is $\pi/2$ ($3\pi/2$), an OAM_{+1} (OAM_{-1}) can be generated. While the phase difference is 0 or 2π, the mode is still a LP_{11} mode.

The experimental setup for the generation and detection of OAM beams using the all-fiber OAM beam converter is sketched in Fig. 6. The output beam from a tunable laser is divided into two paths by a 50:50 optical coupler. One path is used to generate OAM beams and the other path is used as a reference beam to interfere with the generated OAM beam. A SMF as a mode filter (prevents the LP_{11} mode) is directly spliced to the TMF, and the fusion splice between two fibers is shown in the inset. Since the SMF and TMF have similar size and material properties, the fusion splice is pretty smooth, guaranteeing high coupling efficiency and low-mode crosstalk. The splicing loss between the SMF and the TMF is assessed to be less than 0.05 dB. Moreover, to further mitigate the effects of the unwanted LP_{11} mode before the mechanical LPG, a mode stripper realized by the tight bending of the TMF (~16 rounds over 12 mm posts) is used to ensure a pure LP_{01} launching. When varying the pressure applied to the mechanical LPG and adjusting the input polarization by controlling the polarization controller (PC), an input LP_{01} mode [Fig. 7(a)] can be converted to a LP_{11} mode [Figs. 7(b)–7(d)] with high coupling efficiency. Then a rotator is used to align the LP_{11} mode to different directions, as displayed in Figs. 7(b)–7(d). A pair of 75 mm metal flat slabs is used to stress the TMF to produce a phase difference between the two orthogonal LP_{11} modes. By adjusting the pressure to a suitable value, the output beam could be an OAM beam. Finally, the TMF output is collimated using a 20× objective lens and the beam intensity is imaged using a CCD camera. Through the interference pattern between the generated OAM beams and the reference beam, the topological charge number can be identified.

When the TMF is not deformed, the output beam is a Gaussian beam, as displayed in Fig. 7(a). The intensity profiles of the generated LP_{11} modes are shown in Figs. 7(b)–7(d). It can be clearly seen that the intensities present as two side lobe distributions. Moreover, by adjusting the rotator, the output LP_{11} beams can be a LP_{11a}, LP_{11b}, or LP_{11} beam with an arbitrary direction. When the pressure loaded on the metal parallel slab and the direction of the LP_{11} mode (controlled by the rotator) before the parallel slabs are adjusted appropriately, an OAM beam can be achieved at the output terminal of the TMF. The intensity distributions of the generated OAM beams with $l = \pm 1$ are illustrated in Fig. 8. Annular profiles can be clearly seen from Figs. 8(a) and 8(c). In order to confirm the feature of helical phase structure, we interfere the generated OAM beams with a reference-expanded Gaussian beam. The interference patterns are shown in Figs. 8(b) and 8(d). The counterclockwise spiral interference pattern for OAM_{+1} and the clockwise spiral interference pattern for OAM_{-1} can be clearly seen from the figures, which indicate that OAM_{+1} and OAM_{-1} are successfully achieved at the output terminal of the TMF. The obtained results shown in Fig. 8 with

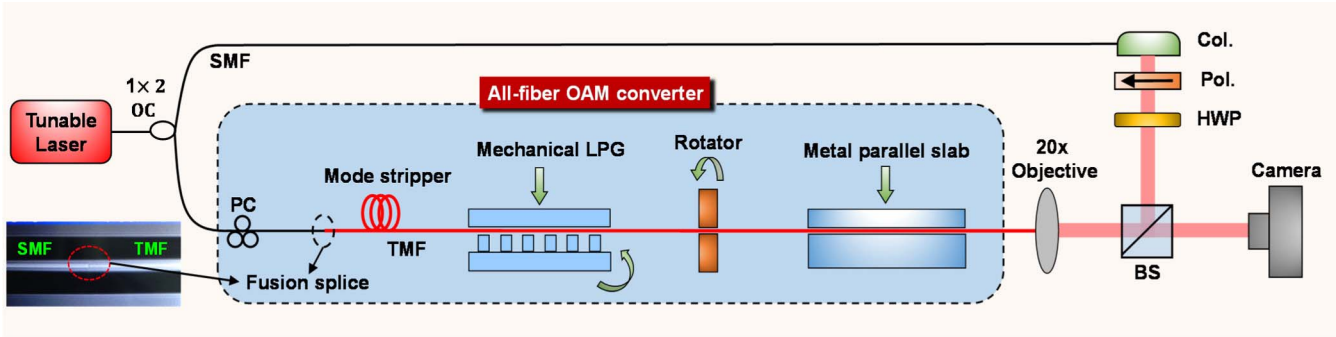

Fig. 6. Experiment setup for the generation and detection of OAM beams using an all-fiber OAM beam converter. OC, optical coupler; PC, polarization controller; SMF, single-mode fiber; TMF, two-mode fiber; LPG, long-period grating; Col., collimator; Pol., polarizer; HWP, half-wave plate; BS, beam splitter.

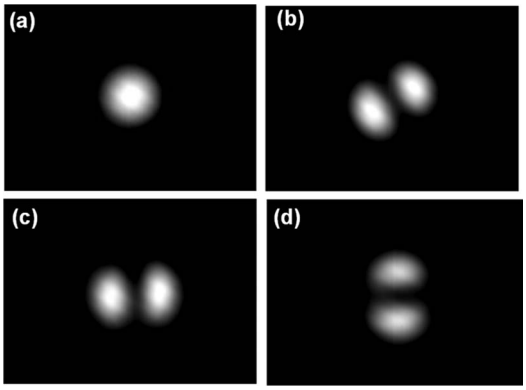

Fig. 7. (a) Intensity profile of the input LP_{01} mode. (b)–(d) Intensity profiles of the LP_{11} modes generated by the LPG and aligned by the rotator.

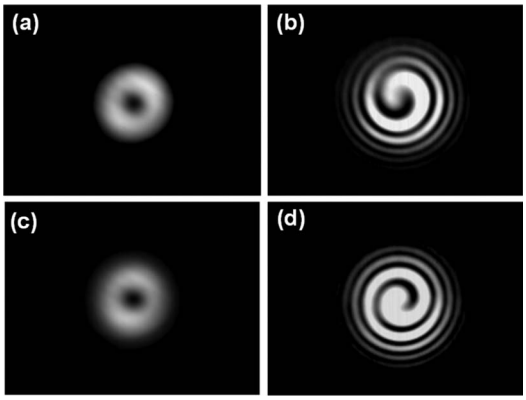

Fig. 8. Intensity profiles of the generated (a) OAM_{-1} and (c) OAM_{+1}. Interference patterns of (b) OAM_{-1} and (d) OAM_{+1} with a reference Gaussian beam (interferograms).

high-quality annular shape intensity profiles and clear interferograms imply high mode purity of the generated OAM beams.

In summary, we have experimentally demonstrated a scalable, controllable, low-cost, and versatile all-fiber OAM converter by deforming a TMF with mechanical devices. Selective generation of the LP_{11a}, LP_{11b}, OAM_{-1}, or OAM_{+1} mode is demonstrated. Since it is an all-fiber device, the converter is compact and compatible with optical fiber communication systems. Moreover, the converter can realize mode switching between LP_{01}, LP_{11a}, LP_{11b}, OAM_{+1}, and OAM_{-1}. With future improvements, in order to enhance the stability of the converter, a permanent LPG can be used to replace the mechanical LPG. The device can also be cured by ultraviolet glue to realize a fixed stable mode conversion, such as LP_{01} to OAM_{+1}. Moreover, an adaptive feedback correction could be used to monitor and compensate any perturbation and stabilize the mode conversion. Additionally, the TMF used in the experiment only supports OAM_{+1} and OAM_{-1}. However, by employing a few-mode fiber which supports more numbers of modes and using a new LPG with an appropriate grating period, the proposed mode converter could also be used to generate higher-order OAM modes. It is believed that manipulating structured light beams with the simple all-fiber device might inspire the development of many fields. The proposed simple, scalable, low-cost, and versatile mode generator may see potential applications in mode-division multiplexing, optical manipulation, and other interesting fields.

Funding. National Basic Research Program of China (973 Program) (2014CB340004, 2014CB340003); National Natural Science Foundation of China (NSFC) (11274131, 11574001, 61222502); Program for New Century Excellent Talents in University (NCET-11-0182); Wuhan Science and Technology Plan Project (2014070404010201); Fundamental Research Funds for the Central Universities (HUST) (2012YQ008); Fundamental Research Funds for the National Laboratory for Optoelectronics (WNLO) (2013ZZGH003); Seed project of Wuhan.

Acknowledgment. The authors would like to thank Jun Liu, Long Zhu, Yifan Zhao, Jing Du, and Liang Fang for technical support and helpful discussions.

REFERENCES

1. D. L. Andrews, *Structured Light and Its Applications: An Introduction to Phase-Structured Beams and Nanoscale Optical Forces* (Elsevier, 2008).
2. A. M. Yao and M. J. Padgett, Adv. Opt. Photon. **3**, 161 (2011).
3. L. Allen, M. W. Beijersbergen, R. J. C. Spreeuw, and J. P. Woerdman, Phys. Rev. A **45**, 8185 (1992).
4. A. Mair, A. Vaziri, G. Weihs, and A. Zeilinger, Nature **412**, 313 (2001).
5. D. Grier, Nature **424**, 810 (2003).
6. S. Furhapter, A. Jesacher, S. Bernet, and M. Ritsch-Marte, Opt. Express **13**, 689 (2005).
7. S. Franke-Arnold, L. Allen, and M. Padgett, Laser Photon. Rev. **2**, 299 (2008).
8. J. Wang, J. Yang, I. M. Fazal, N. Ahmed, Y. Yan, H. Huang, Y. Ren, Y. Yue, S. Dolinar, M. Tur, and A. E. Willner, Nat. Photonics **6**, 488 (2012).
9. N. Bozinovic, Y. Yue, Y. Ren, M. Tur, P. Kristensen, H. Huang, A. E. Willner, and S. Ramachandran, Science **340**, 1545 (2013).
10. H. Huang, G. Xie, Y. Yan, N. Ahmed, Y. Ren, Y. Yue, D. Rogawski, M. J. Willner, B. I. Erkmen, K. M. Birnbaum, S. J. Dolinar, M. P. J. Lavery, M. J. Padgett, M. Tur, and A. E. Willner, Opt. Lett. **39**, 197 (2014).
11. J. Wang, S. Li, M. Luo, J. Liu, L. Zhu, C. Li, D. Xie, Q. Yang, S. Yu, J. Sun, X. Zhang, W. Shieh, and A. E. Willner, *Proceedings of European Conference and Exhibition on Optical Communication (ECOC)* (IEEE, 2014), paper Mo.4.5.1.
12. S. Li and J. Wang, Sci. Rep. **4**, 3853 (2014).
13. L. Marrucci, C. Manzo, and D. Paparo, Phys. Rev. Lett. **96**, 163905 (2006).
14. G. Gibson, J. Courtial, M. J. Padgett, M. Vasnetsov, V. Pas'ko, S. M. Barnett, and S. Franke-Arnold, Opt. Express **12**, 5448 (2004).
15. Z. Zhao, J. Wang, S. Li, and A. E. Willner, Opt. Lett. **38**, 932 (2013).
16. X. Cai, J. Wang, M. J. Strain, B. Johnson-Morris, J. Zhu, M. Sorel, J. L. O'Brien, M. G. Thompson, and S. Yu, Science **338**, 363 (2012).
17. D. McGloin, N. B. Simpson, and M. J. Padgett, Appl. Opt. **37**, 469 (1998).
18. P. Z. Dashti, F. Alhassen, and H. P. Lee, Phys. Rev. Lett. **96**, 043604 (2006).
19. S. Ramachandran, P. Kristensen, and M. F. Yan, Opt. Lett. **34**, 2525 (2009).
20. Y. Yan, L. Zhang, J. Wang, J.-Y. Yang, I. M. Fazal, N. Ahmed, A. E. Willner, and S. J. Dolinar, Opt. Lett. **37**, 3294 (2012).
21. I. Giles, A. Obeysekara, R. Chen, D. Giles, F. Poletti, and D. Richardson, IEEE Photon. Technol. Lett. **24**, 1922 (2012).
22. S. Ramachandran, Z. Wang, and M. Yan, Opt. Lett. **27**, 698 (2002).
23. L. Grüner-Nielsen and J. W. Nicholson, *Proceedings of IEEE Summer Topical Meeting* (IEEE, 2012), paper WC1.2.
24. Y. Gu, K. S. Chiang, and Y. J. Rao, IEEE Photon. Technol. Lett. **21**, 657 (2009).